

Effect of Dioctyl Sebacate on Corrosion Behavior of Fine-grain High-strength Reinforcement in Simulated Concrete Pore Solutions

Bilan Lin^{1,2,*}, Zan Luo¹, Chaonong Liu¹, Xuefeng Liu¹ and Yuye Xu³

¹ School of Material Science and Engineering, Xiamen University of Technology, Xiamen 361024, China

² Key Laboratory of Functional Materials and Applications of Fujian Province, Xiamen 361024, China

³ College of Civil Engineering, Huaqiao University, Xiamen, Fujian 361021, China

*E-mail: linbilan@xmut.edu.cn

Received: 1 July 2017 / *Accepted:* 12 August 2017 / *Published:* 12 September 2017

Dioctyl sebacate (DS) was used as a corrosion inhibitor for fine-grain high-strength reinforcement (HRBF500 reinforcement) in simulated concrete pore solutions (SCP solutions) with 3.5% NaCl. The corrosion behavior of HRBF500 reinforcement was investigated using potentiodynamic polarization curves, electrochemical impedance spectroscopy (EIS) diagrams, Mott-Schottky curves and scanning electron microscopy (SEM) observations. Comparisons were made with plain carbon steels (HPB300 reinforcement). In addition, the corrosion inhibition effect of the composite inhibitor, DS and molybdate, was studied. The results show that the cathodic corrosion process of HRBF500 is greatly inhibited by DS, which acts as a cathodic inhibitor. With an increase in DS content, the corrosion current density decreases and the electrochemical impedance increases; a reduction in donor concentration of the corrosion product membrane occurs. The corrosion of the HRBF500 reinforcement is substantially inhibited but not eliminates. A suitable DS concentration was approximately 2.0%. Compared to HRBF500, for HPB300 reinforcement with 2% DS, the anodic polarization curve exhibits a passivation region, the impedance is considerably higher, and the corrosion almost disappears. The corrosion inhibition efficiency of DS is superior for HPB300 than that for HRBF500. Moreover, regarding the composite inhibitor of DS and molybdate, a synergistic inhibitive effect is well exerted. The corrosion protection efficiency for HRBF500 reinforcement is up to 99.3%, and the corrosion current density is decreased to $0.08 \mu\text{A}\cdot\text{cm}^{-2}$, for more than two orders of magnitude.

Keywords: Reinforcement; Fine grain; Corrosion; Inhibitor; Simulated concrete pore solution; Dioctyl sebacate; Molybdate

1. INTRODUCTION

HRBF500 reinforcement refers to the Hot-rolled Ribbed Bar with Fine grains and with a yield strength grade of 500 MPa. Based on the plain carbon steel (HPB300 reinforcement, i.e. Hot-rolled Plain Bar with a yield strength grade of 300 MPa) and 20MnSi steel (HRB335 reinforcement, i.e. Hot-rolled Ribbed Bar with a yield strength grade of 335 MPa), HRBF500 reinforcement is developed through the optimization of the micro alloying elements (V, Nb, Ti) and the thermo mechanical control process (TMCP) where the grains are refined and the microscopic structures are improved. Both the strength and ductile plasticity of HRBF500 reinforcement are enhanced, meeting the evolving demands of society and the built environment. According to the current Chinese national standard, "Code for design of concrete structures (GB50010-2010)", HRBF500 reinforcement has become one of the leading stress reinforcement strategies for reinforced concrete structures in China. However, despite the extensive application of HRBF500 reinforcement, there are few studies reported concerning the corrosion resistance properties of these high-performance steels.

Recently, the corrosion and protection of reinforced concrete media have been studied widely [1-5], but work is focused mainly on the traditional reinforcement such as HPB300 and HRB335. However, an increase in strength of reinforcement is likely to bring about a reduction in corrosion properties [6-11]. Shi et al. [12, 13] found that pitting corrosion of HRB500E steel with fine grains is more serious than that for the carbon steel in alkaline environments containing chloride ions, and pointed out that the number of the grain boundaries and the trace elements are the main causes of the lower corrosion resistance of HRB500E. In previous studies, the corrosion sensitivity of HRB500 reinforcement to chloride ions is more serious than that of HPB300 [14] and the inhibition efficiency of nitrite for HPB300 is superior to that for HRBF500 [15]. Also, phosphate and sodium D-gluconate have been shown to suppress the corrosion of HRBF500 [16, 17], similar to that reported for carbon steel [18-20]. However, some corrosion inhibitors such as phytic acid and benzotriazole, which are effective to HPB300 reinforcement, are invalid for HRBF500 [17-22]. Therefore, to ensure the durability and safety of the concrete engineering structures, the corrosion behavior of HRBF500 reinforcement should be studied in a systematic manner.

Corrosion inhibitor is one of effective protection measures to reinforcement and has been widely used in reinforced concrete structures [23-26]. Due to economy, availability and degradability [27-29], dioctyl sebacate (DS) recently has been tried to use as a corrosion inhibitor for reinforcement [30-33]. Wang et al. [30, 31] studied the effect of DS on the electrochemical properties of HPB300 reinforcement in SCP solutions containing chloride ions, and found that a sedimentation film is formed on the substrate surface, inhibiting the anodic corrosion process. Du et al. [32, 33] developed a composite corrosion inhibitor containing DS, sodium D-gluconate and zinc sulfate, and found that the composite inhibitor can restrain both the anodic and the cathodic corrosion processes of HPB300 in SCP solutions and concrete blocks, and a good synergistic inhibition effect is exerted [32, 33]. In the afore-mentioned study, the mass content of DS is up to 70–85% [33].

Molybdate is a commonly used anodic corrosion inhibitor for metal materials and a molybdate passivation film is formed on the surface of the metal [34-36]. In recent years, molybdate has also been used as a corrosion inhibitor for carbon steel reinforcement [37-39], which an improved corrosion

inhibiting effect occurs, reflecting an enhancement in compactness and stability of the passivation film [35]. Furthermore, in the context of repairing pitting corrosion, molybdate is better than nitrite [39].

In this study, the corrosion inhibition effect of DS for HRBF500 reinforcement in SCP solutions containing 3.5% NaCl will be investigated using electrochemical measurements and SEM observations. Comparative studies between HRBF500 and HPB300 reinforcements will also be performed and the effect of the composite inhibitor of DS and molybdate on the electrochemical corrosion behavior of HRBF500 reinforcement is considered.

2. EXPERIMENTAL

2.1 Materials and reagents

The tested samples were HRBF500 and HPB300 reinforcements with corresponding diameters of 16 mm and 12 mm, respectively. One end of the sample was served as the working surface and other parts were sealed with epoxy resin. Thus, the working surface areas of the HRBF500 and HPB300 samples were 2.01 cm^2 and 1.13 cm^2 , respectively.

A saturated calcium hydroxide solution was served as the SCP solution. The pH value is about 12.5. Sodium chloride with mass fraction of 3.5% was added into SCP solutions to simulate the invasion of chloride ions. The mass fraction of DS inhibitor was 0%, 0.75%, 1.0%, 1.5% and 3.0%, respectively. Molybdate was introduced by sodium molybdate dehydrate, of which the mass concentration was 0.4 g/L. All chemical reagents were of analytical grade and all test solutions were prepared with distilled water.

2.2 Electrochemical measurements

Electrochemical measurements consisted of potentiodynamic polarization curves, electrochemical impedance spectroscopy (EIS) diagrams and Mott-Schottky curves. All electrochemical tests were carried out using a CHI604E electrochemical workstation. The test cell was a conventional three-electrode system, i.e. reference electrode, auxiliary electrode and working electrode, of which were served by the saturated calomel electrode (SCE), platinum electrode and the tested reinforcement, respectively. All potentials below were relative to the SCE.

Before electrochemical measurements, the working surface of the reinforcement samples was successively polished with sandpapers of 200# to 2000# grade. Then the sample was scrubbed with acetone, rinsed with distilled water and dried with cool air. Thereafter, the test sample was immersed in quiescent SCP solutions for about one hour to obtain a steady open circuit potential.

The potentiodynamic polarization curves were measured from the cathodic direction to the anodic direction and were stopped when the anodic current increased rapidly. Here the initial cathodic potential was the steady open circuit potential minus 0.3 V. The scan rate was 1 mV/s. The corrosion current density i_{corr} , the corrosion potential E_{corr} , the anodic Tafel slope b_a and the cathodic Tafel slope b_c were obtained from the measured polarization curves. The corrosion protection efficiency P_e of DS for HRBF500 reinforcement was calculated from the following expression

$$P_e(\%) = \left(1 - \frac{i_{\text{cor}}}{i_{\text{cor}}^0}\right) \times 100 \quad (1)$$

Where i_{cor}^0 and i_{cor} were the corrosion current densities of the HRBF500 samples without and with DS inhibitor, respectively. Furthermore, the polarization control type of the DS inhibitor was also analyzed according to the Evans polarization principle [40]. On the assumption that the ohmic resistance of the whole system was negligible [15], the control degree of the anodic and cathodic polarization, i.e. C_a and C_c , were calculated as follows:

$$C_a(\%) = \frac{b_a}{(b_a + b_c)} \times 100 \quad (2)$$

$$C_c(\%) = \frac{b_c}{(b_a + b_c)} \times 100 \quad (3)$$

When C_a is much greater than C_c , it indicates that DS acts mainly as an anodic corrosion inhibitor. Conversely, DS acts mainly as a cathodic inhibitor.

EIS diagrams were performed at the above steady open circuit potential. The frequency range was from 100 kHz to 0.01 Hz. The amplitude of the AC voltage was 5 mV.

Mott-Schottky curves were recorded to investigate the semiconductor characteristics of the corrosion product membrane formed on the surface of the reinforcement. The potential ranged from -0.6 V to 0.4 V. The frequency was 1 kHz. The amplitude and the interval of the AC signal was 10 mV.

To ensure the reliability of the experimental results, each set of the specimens was tested three to five times.

2.3 Corrosion morphology analysis

After the test samples underwent corrosion, the surface morphology was recorded using SEM (EVO-18, Zeiss). The chemical composition of the corrosion products was determined by energy-dispersive X-ray spectroscopy (EDS) (X-MAX 20, Oxford Instruments).

3. RESULTS AND DISCUSSION

3.1 Corrosion inhibition effect of DS for HRBF500 - potentiodynamic polarization curves

Figure 1 shows the effect of the DS inhibitor on the potentiodynamic polarization curves for the HRBF500 samples in SCP solutions containing 3.5% NaCl. The corresponding corrosion parameters are listed in Table 1.

As can be seen in Fig. 1, irrespective of whether the SCP solutions with 3.5% NaCl contained DS or not, both the anodic and the cathodic corrosion processes of HRBF500 reinforcement are controlled by the activation polarization. That is, the loss of the electrons at the anode iron and the consumption of the electrons by the dissolved oxygen at the cathode are the controlling steps for the corrosion reactions. When DS was added to the SCP solutions, both the anodic and the cathodic polarization curves are shifted to the left with different degrees. That is, the anodic and cathodic polarization currents are decreased with various extents. These indicate that the corrosion processes at

the anode and the cathode are inhibited differently by DS. With an increase in DS content from 0% to 0.75%, the cathodic polarization curves are obviously shifted to the left, while the anodic curves show minimal variation, suggesting that the DS inhibitor with 0.75% content mainly suppresses the cathodic corrosion process. This may reflect the fact that DS is preferentially adsorbed onto the active cathode sites of the HRBF500 samples which thus inhibits the reduction reaction of the oxygen atom at the cathode. Increasing DS content to 1.5%, the cathodic polarization curve continues shifting to the left while the anodic curve moves left only slightly. It implies that for a large addition of DS inhibitor, the cathodic active sites for the HRBF500 samples are further covered and a part of the anodic surface is also covered. When the concentration of DS was increased to 2.0%, change in the cathodic curve is not evident, while the anodic curve is greatly left-shifted. The latter implies that the anodic areas are covered continuously. However, with 3.0% DS, both the cathodic and the anodic polarization branches are shifted to the right. Namely, an excessive concentration of DS is not favorable for the corrosion inhibition for HRBF500 reinforcement. This may be associated with a decrease in pH value of the SCP solutions with more DS.

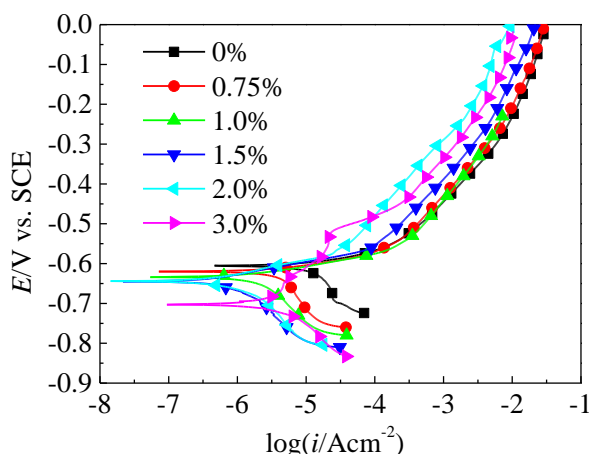


Figure 1. Effect of DS content on the polarization curves for HRBF500 in SCP solutions containing 3.5% NaCl

Table 1. Effect of DS content on corrosion parameters for HRBF500 obtained from Fig. 1

| DS content/ wt. % | $i_{corr}/\mu A \cdot cm^{-2}$ | E_{corr}/V | $b_a/mV \cdot dec^{-1}$ | $b_c/mV \cdot dec^{-1}$ | $C_a/\%$ | $C_c/\%$ | $P_c/\%$ |
|----------------------|--------------------------------|--------------|-------------------------|-------------------------|----------|----------|----------|
| 0 | 12.3 | -0.605 | 134 | 142 | 48.6 | 51.4 | — |
| 0.75% | 3.94 | -0.620 | 130 | 211 | 38.1 | 61.9 | 68.0 |
| 1.0% | 1.43 | -0.634 | 105 | 168 | 38.5 | 61.5 | 88.4 |
| 1.5% | 0.52 | -0.645 | 100 | 177 | 36.1 | 63.9 | 95.8 |
| 2.0% | 0.45 | -0.644 | 116 | 202 | 36.5 | 63.5 | 96.3 |
| 3.0% | 1.93 | -0.700 | 110 | 166 | 39.9 | 60.1 | 84.3 |

As shown in Fig. 1, there is no passivation interval on the anodic polarization curves and the corrosion potential, E_{corr} , moves in a negative direction. It can be surmised that the corrosion inhibition

for HRBF500 reinforcement by DS is achieved not through the anodic passivation, but through an adsorption membrane which preferentially adsorbs on the active cathode sites. This is different from the corrosion inhibition effect of sodium D-gluconate, nitrite and phosphate for HRBF500 reinforcement, where there are passivation regions on the anodic polarization curves [15-17].

As shown in Table 1, with an increase in DS content in the SCP solutions containing 3.5% NaCl, the corrosion current density, i_{corr} , of HRBF500 reinforcement first decreases significantly and then slightly increases; the corrosion protection efficiency, P_e , first increases dramatically and then decreases. The optimum content of DS inhibitor was about 2.0%, whereby i_{corr} decreases from $12.3 \mu\text{A}\cdot\text{cm}^{-2}$ to $0.45 \mu\text{A}\cdot\text{cm}^{-2}$ and P_e is up to 96.3%. In the presence of DS, the anodic Tafel slope, b_a , declines for different extents while the cathodic Tafel slope, b_c , is enhanced with various degrees. The b_c value is clearly larger than b_a , resulting in a markedly larger C_c value compared to C_a . Therefore, the cathodic polarization control of the corrosion processes of HRBF500 reinforcement is dominant, and DS plays as a cathodic corrosion inhibitor. This is different from the results of Wang et al. [30, 31], where DS acts as an anodic corrosion inhibitor for HPB300. Furthermore, E_{corr} of the HRBF500 samples decreases with an increase in DS content. This is also due to that the action of the cathodic polarization is greater than that of the anodic polarization. Moreover, according to the Evans polarization mechanism, a drop of i_{corr} and a negative shift of E_{corr} of HRBF500 reinforcement are also attributed to a decrease of b_a and an increase of b_c , after addition of DS inhibitor.

3.2 Corrosion inhibition effect of DS for HRBF500 - EIS diagrams

Figure 2 presents the effect of the DS inhibitor on the EIS diagrams (including the Nyquist and Bode diagrams) for HRBF500 reinforcement in SCP solutions containing 3.5% NaCl. In the absence of DS, the Nyquist impedance spectrum for HRBF500 is very small (Fig. 2 (a)). That is, the electrochemical impedance value is exceedingly small. However, in the presence of DS, the impedance values are markedly enhanced. In fact, the values greatly improve at first and then drop slightly with an increase in DS content. The impedance is at a higher level when the DS content was about 1.5–2.0%. Similarly, the impedance modulus for HRBF500 first increases and then decreases with an increase in DS content (Fig. 2 (b)).

As shown in Fig. 2 (c), in the absence of DS, the peak of the negative phase angle is small and the frequency range of the peak is narrow. With an increase in DS content, the peak of the negative phase angle first obviously increases and then decreases slightly, and the frequency range of the corresponding peak is first moved to the low frequency end and then slightly shifted to the high frequency end.

In the actual corrosion system, the double layer capacitor of the interface between the HRBF500 sample and the SCP solution has a great difference from the ideal plate capacitor. Thus, the semicircle arc corresponding to the capacitive loop in the Nyquist diagrams is deformed and the peak value of the negative phase angle deviates from 90° [41, 42]. The greater the difference is between the actual and the ideal capacitors, the larger will be the deformation of the semicircle arc, and the farther away from 90° will be the peak of the negative phase angle. This deviation degree is closely associated with the compactness and roughness of the corrosion products on the surface of the metals [43, 44]. If

the corrosion products are smoother and more compact, the actual double layer capacitor will be closer to the ideal plate capacitor, so the peak value of the negative phase angle is more and more approached to 90°.

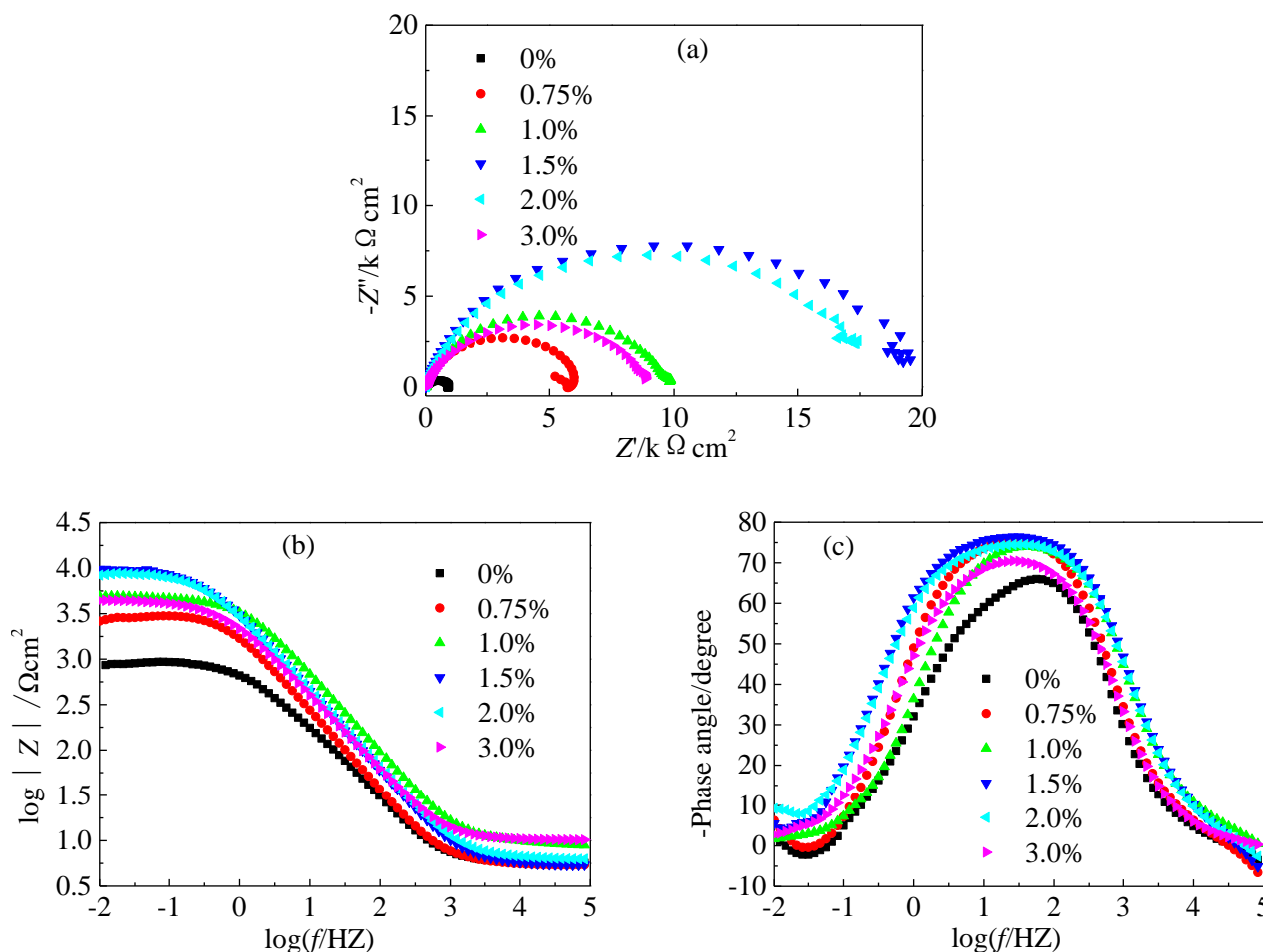


Figure 2. Effect of DS content on the Nyquist (a) and Bode (b) (c) diagrams for HRBF500 in SCP solutions containing 3.5% NaCl

Therefore, a larger peak value of the negative phase angle indicates a better corrosion protection of the corrosion product membrane on the surface of reinforcement. It should be pointed out that the maximum peak value of the negative phase angle cannot exceed 90° [41].

Moreover, the larger the frequency range is, corresponding to the negative phase angle peak, the smaller the capacitance value of the corresponding capacitor [40, 45, 46]. Thus, the surface corrosion products will be more compact and thicker, exhibiting an enhanced corrosion protection performance. This is due to that the capacitance of a capacitor is proportional to the surface area of the plates and inversely proportional to the distance between the two plates [47]. When the corrosion products are more compact and smoother, the surface area of the capacitor plate will be smaller. Similarly, when the corrosion products are thicker, the distance between the two plates will be larger. For such scenarios, the capacitance will be smaller, which will correspond to a larger frequency range of the negative phase angle peak in the Bode diagrams.

The above EIS results show that the corrosion resistance of HRBF500 reinforcement is remarkably enhanced with the addition of DS to the SCP solutions containing 3.5% NaCl. This enhanced performance is intimately linked with the formation of the corrosion products which are relatively thick and compact. An appropriate concentration for the DS inhibitor is 1.5–2.0%.

3.3 Corrosion inhibition effect of DS for HRBF500 - Mott-Schottky curves

Generally, the corrosion products on the surface of the metals have semiconducting properties. According to the Mott-Schottky theory [48, 49], the relationships of the different types of semiconductors are as follows:

$$n\text{-type: } \frac{1}{C_{sc}^2} = \frac{2}{\varepsilon_0 \varepsilon e N_D} \left[E - E_{fb} - \frac{kT}{e} \right] \quad (4)$$

$$p\text{-type: } \frac{1}{C_{sc}^2} = -\frac{2}{\varepsilon_0 \varepsilon e N_A} \left[E - E_{fb} - \frac{kT}{e} \right] \quad (5)$$

Where C_{sc} is the capacitance of the corrosion product membrane when the space charge was exhausted, E is the electrode potential, ε_0 is the dielectric constant (8.854×10^{-12} F/m) in vacuum, ε is the relative dielectric constant of the corrosion product membrane (12 [49]), e is the electron charge (1.602×10^{-19} C), N_D and N_A are the donor concentration and the acceptor concentration of the corrosion product membrane, respectively, E_{fb} is the flat band potential, K is the Boltzmann constant (1.38066×10^{-23} J/K) and T is the thermodynamic temperature. When the slope of the Mott-Schottky curve is positive, the corrosion product membrane is an n -type semiconductor. Otherwise, it is a p -type semiconductor. At room temperature, kT/e is about 25 mV, which for the present experiments can be neglected. Therefore, according to the slope of the Mott-Schottky curve, the N_D or N_A values can be obtained.

Figure 3 shows the effect of DS content on the Mott-Schottky curves for HRBF500 reinforcement in SCP solutions containing 3.5% NaCl. Irrespective of whether DS was added into, the slope of the Mott-Schottky curves in the lower potential range is positive. It suggests that the corrosion products formed on the HRBF500 samples are n -type semiconductor. There are two straight lines in all curves, corresponding to the low potential in the range from approximately -0.60 V to -0.45 V and the high potential ranged from -0.30 V to -0.15 V, respectively. This implies that there are two donor concentrations in the corrosion products of HRBF500 reinforcement [49].

The previous studies have shown that there are double layer structures in the membrane formed on the surface of iron in strongly alkaline environments [39, 50, 51]. The inner layer is Fe_3O_4 and the outer layer is $\gamma\text{-}Fe_2O_3$. Fe^{2+} in Fe_3O_4 more readily forms the soluble salts or complexes than Fe^{3+} in Fe_3O_4 and $\gamma\text{-}Fe_2O_3$ [39]. Hence, the corrosion resistance of the corrosion product membrane will be impaired by Fe^{2+} and a less content of Fe^{2+} will provide more excellent anti-corrosion performance. However, a higher content of chloride ions in the SCP solutions will lead to an increase in Fe^{2+} and a decrease in Fe^{3+} in the formed corrosion products [52]. Namely, chloride ions will impair the corrosion resistance of the metals.

Therefore, the conductive carriers in the low potential region are mainly the oxygen holes and Fe^{2+} , denoted by the shallow donor concentration N_{D1} . Those in the high potential region are mainly the oxygen holes and Fe^{3+} , denoted by the deep donor concentration N_{D2} [49]. A higher content of Fe^{3+} will generate a lower content of oxygen holes and a smaller N_{D2} , resulting in a better corrosion resistance of the corrosion products. Conversely, the corrosion resistance of HRBF500 reinforcement is poorer.

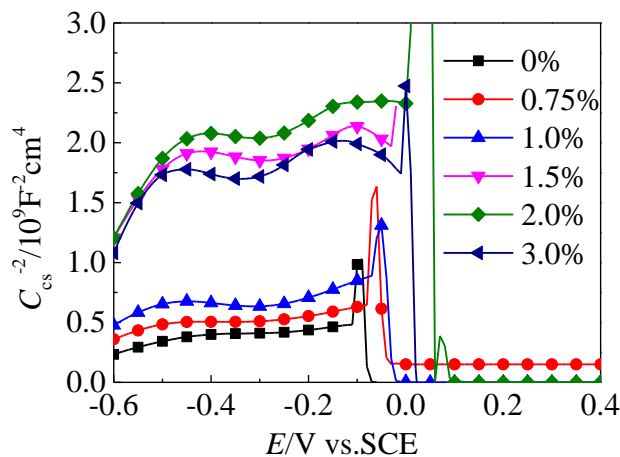


Figure 3. Effect of DS content on the Mott-Schottky curves for HRBF500 in SCP solutions containing 3.5% NaCl

As shown in Fig. 3, when the electrode potential E exceeded a certain value, there is a discontinuous change in the Mott-Schottky curves. This is due to that an excessive electrode potential will retard the oxidation of Fe^{2+} to Fe^{3+} in the inner layer of the corrosion product membrane, leading to a depletion of the donor concentration [39]. Therefore, the properties of n -type semiconductors cannot be demonstrated. In other words, when the electrode potential corresponding to a discontinuous change is high; the Fe^{3+} content will also be high and the protection of the corrosion product membrane will be further enhanced. When the DS content was 2.0%, the electrode potential for a discontinuous change is biggest, so the corresponding corrosion resistance of HRBF500 reinforcement is maximized.

Table 2. Effect of DS content on N_{D1} and N_{D2} of the corrosion products on HRBF500

| DS content/wt.% | $N_{D1}/(\times 10^{19} \text{ cm}^3)$ | $N_{D2}/(\times 10^{19} \text{ cm}^3)$ |
|-----------------|--|--|
| 0 | 11.4 | 30.4 |
| 0.75 | 6.85 | 8.94 |
| 1.0 | 3.51 | 9.94 |
| 1.5 | 1.66 | 4.96 |
| 2.0 | 1.81 | 5.31 |
| 3.0 | 2.03 | 6.02 |

Table 2 lists the shallow and deep donor concentrations N_{D1} and N_{D2} of the corrosion products on the surface of the HRBF500 samples. When DS was added to the SCP solutions containing 3.5% NaCl, both the N_{D1} and N_{D2} values of the corrosion products greatly decrease, leading to an improvement of the corrosion resistance of HRBF500 reinforcement. With an increase in DS content, the N_{D1} and N_{D2} values first markedly decrease and then slightly increase. The N_{D1} and N_{D2} values fall by nearly an order of magnitude when the DS content was about 1.5–2.0%.

3.4 Corrosion inhibition effect of DS for HRBF500 - corrosion morphology

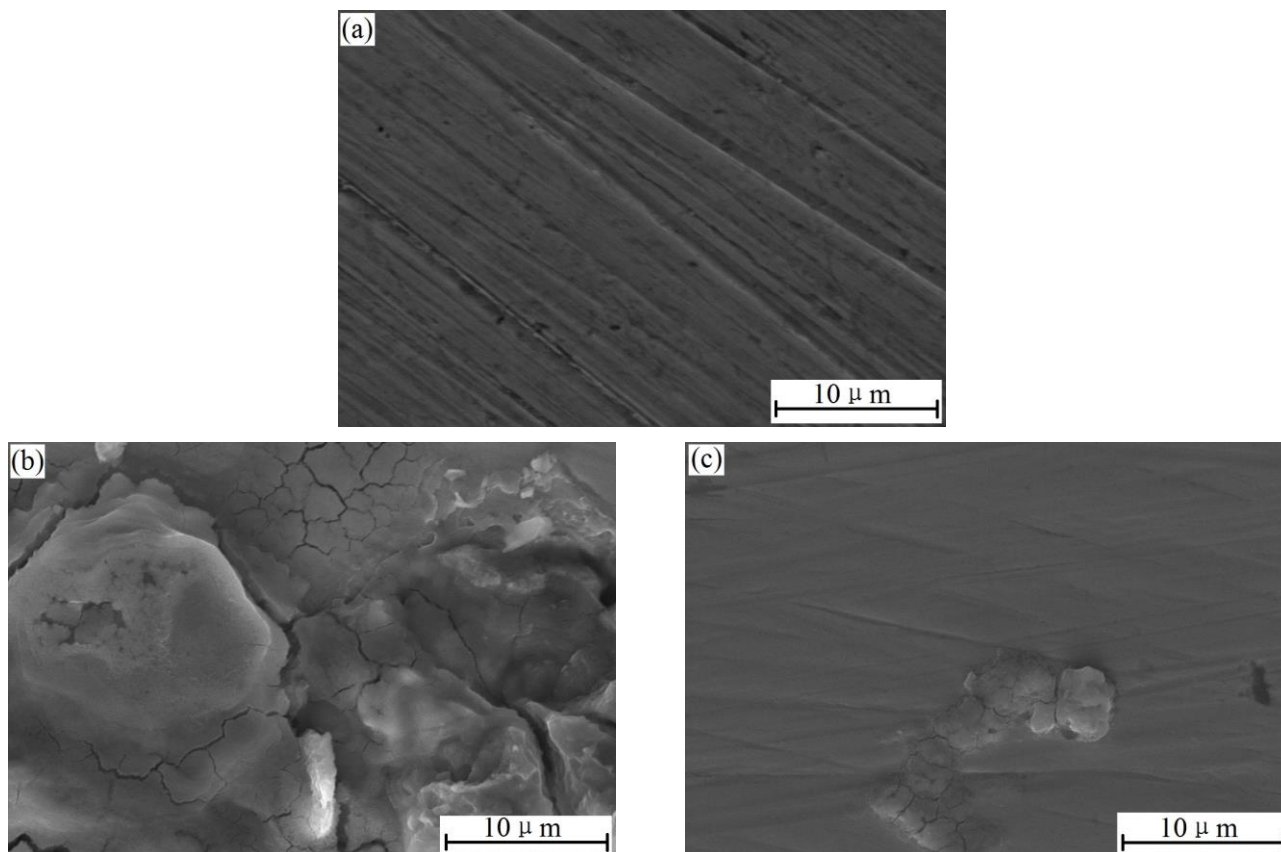


Figure 4. Corrosion morphology of HRBF500 reinforcement immersed in SCP solutions: uncontaminated (a), with 3.5% NaCl (b), with 3.5% NaCl and 2% DS (c)

Figure 4 shows the corrosion morphology of the HRBF500 samples immersed in different SCP solutions. In pure and uncontaminated SCP solution, the surface of HRBF500 is smooth; there are no corrosion pits or corrosion products (Fig. 4 (a)). A stable passivation film is formed on the surface of HRBF500 under conditions of high alkalinity without chloride ions. According to the EDS results, the passivation film is composed mainly of oxygen and iron, as reported in a previous study [15].

When 3.5% NaCl was added to SCP solution, the HRBF500 sample suffers serious corrosion (Fig. 4 (b)). Coarse and cracked corrosion products form over the whole surface. The membrane is severely discontinuous and non-compact in nature. Therefore, the corrosion resistance of the HRBF500 sample is very poor, as shown by the above electrochemical data (Figs. 1–3 and Tables 1–

2). The EDS analysis confirms that a high content of chloride is present in the membrane. The participation of chloride in the formation of the corrosion product membrane makes a poor corrosion resistance capability [15].

When 2% DS was added to the SCP solutions containing 3.5% NaCl, the corrosion of the HRBF500 sample is outstandingly inhibited (Fig. 4 (c)). However, a few cracked corrosion products are still formed. It indicates that the corrosion inhibition efficiency of DS for HRBF500 reinforcement is somewhat limited. To improve further the corrosion resistance of HRBF500, other corrosion inhibitors or composite corrosion inhibitors should be investigated.

3.5 Comparison of corrosion inhibition effect of DS for HPB300 and HRBF500

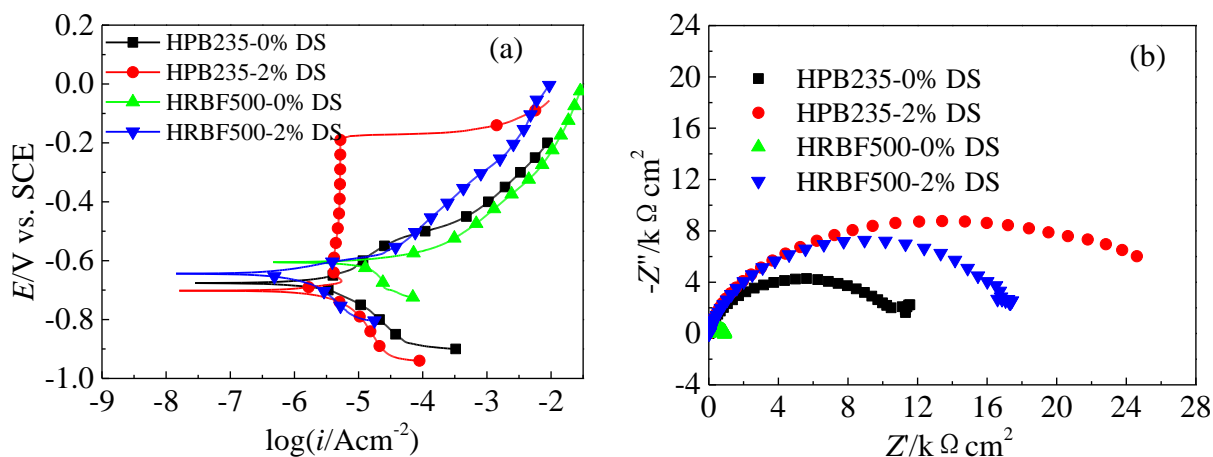


Figure 5. Effect of 2% DS on the polarization curves (a) and Nyquist diagrams (b) for HPB300 and HRBF500 reinforcements in SCP solutions with 3.5% NaCl

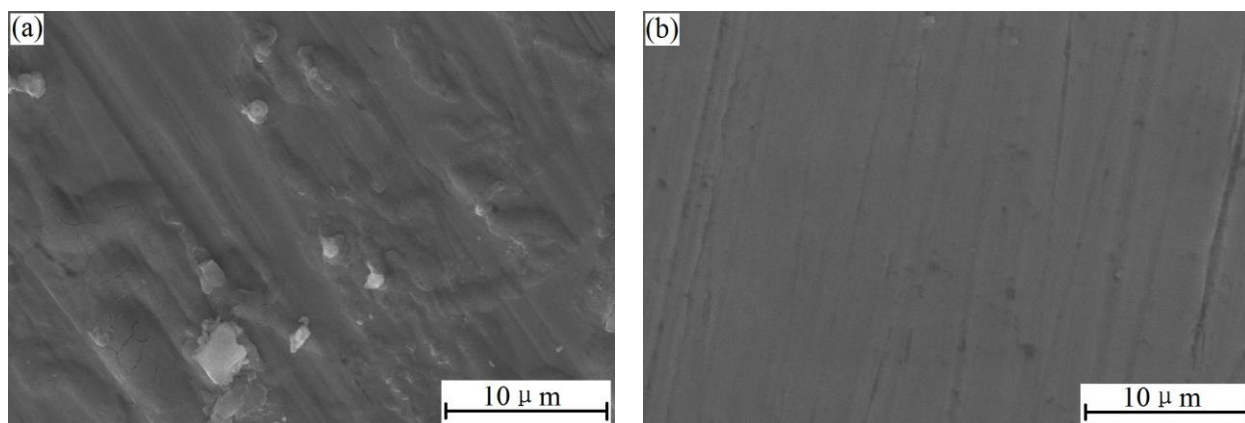


Figure 6. Corrosion morphologies of HPB300 in SCP solutions containing 3.5% NaCl: without DS (a) and with 2% DS (b)

As mentioned in the Introduction section, the corrosion behaviors of HRBF500 and HPB300 reinforcements are different [12-22]. Thus, it is necessary to compare the corrosion inhibition effect of

2% DS for HPB300 and HRBF500. In Figure 5, the effect of 2% DS on the polarization curves and Nyquist diagrams for HPB300 and HRBF500 in the SCP solutions containing 3.5% NaCl are presented. And Figure 6 shows the corrosion morphology of HPB300.

As shown in Fig. 5, in the absence of DS, the anodic and cathodic polarization curves for the HPB300 samples are also characterized by the active polarization, similar to those for HRBF500 (Fig. 1). However, the two polarization curves for HPB300 are on the left of those for HRBF500, respectively. That is, the polarization current of HPB300 is smaller than that of HRBF500. Moreover, the electrochemical impedance value of the former is significantly larger than that of the latter. It can be concluded that the corrosion resistance of HPB300 in SCP solutions containing 3.5% NaCl is superior to that of HRBF500. This is also consistent with the corrosion morphologies presented in Figs. 6(a) and 4(b). The corrosion products on the surface of HPB300 are obviously less than those on HRBF500.

As shown in Figs. 5 and 6, in the presence of 2% DS, the anodic and cathodic polarization curves for HPB300 are outstandingly shifted towards the left, and there is a passivation region on the anodic curve. The DS inhibitor causes a significant decrease in the polarization current and promotes the passivation of HPB300. Moreover, a large fall in the corrosion current density occurs and the electrochemical impedance is enhanced. With respect to the surface morphology, corrosion pits and/or corrosion products on HPB300 are much fewer in number. All these support the contention that 2% DS has a very effective corrosion inhibition for HPB300 in SCP solutions containing 3.5% NaCl.

As far as the comparative studies were concerned, the corrosion resistance indexes of HPB300 are clearly better than those of HRBF500 under the same experimental conditions. Thus, it can be concluded that HPB300 exhibits a better corrosion resistance than HRBF500 in SCP solutions containing 3.5% NaCl whether or not it contains 2% DS.

3.6 Corrosion inhibition effect of the composite inhibitors of DS and molybdate for HRBF500

The above studies demonstrate that the corrosion inhibition efficiency of DS has limitations when it was singly applied to HRBF500 reinforcement. In a further study, the corrosion inhibition effect of a composite inhibitor, 2% DS and 0.4 g/L sodium molybdate, will be evaluated for HRBF500. The polarization curves, the EIS diagrams and the Mott-Schottky curves are shown in Figure 7.

As shown in Fig. 7 (a), when 0.4 g/L sodium molybdate was added to the SCP solution containing 3.5% NaCl, the cathodic polarization curve for HRBF500 is changed little, while the anodic curve is shifted appreciably to the left. Clearly the corrosion potential is shifted in a positive direction. This proves that molybdate functions as an anodic corrosion inhibitor [34-36]. When 2% DS and 0.4 g/L sodium molybdate were used as a composite inhibitor for HRBF500, the cathodic polarization curve is left-shifted significantly, compared to those in SCP solutions without addition of inhibitor or with 0.4 g/L sodium molybdate. However, the differences in the cathodic curves for the composite inhibitor and DS alone are minimal. It indicates that the composite inhibitor retains the corrosion inhibition characteristics of DS. That is, the composite indicator controls significantly the cathodic corrosion of HRBF500. Moreover, comparing the results for the composite inhibitor with those for the

single DS or molybdate inhibitor, the anodic polarization curve for the composite inhibitor is also appreciably left-shifted. It indicates that the combined effect of the two single inhibitors on the anodic corrosion inhibition has been further exploited.

The i_{corr} values of HRBF500 in the presence of the single molybdate and the composite inhibitor are 4.08 and 0.08 $\mu\text{A}\cdot\text{cm}^{-2}$, respectively. Therefore, the corresponding corrosion protection efficiencies, $P_{e,Mo}$ and $P_{e,com}$, are 66.8% and 99.3%, respectively. Assuming that the corrosion inhibition effects of DS and molybdate were independent of each other, the theoretical protection efficiency of the composite inhibitor, $P_{e,the}$, can be calculated by the following expression [53]:

$$P_{e,the} = P_{e,Mo} + P_{e,DS} - P_{e,Mo} \times P_{e,DS} \quad (6)$$

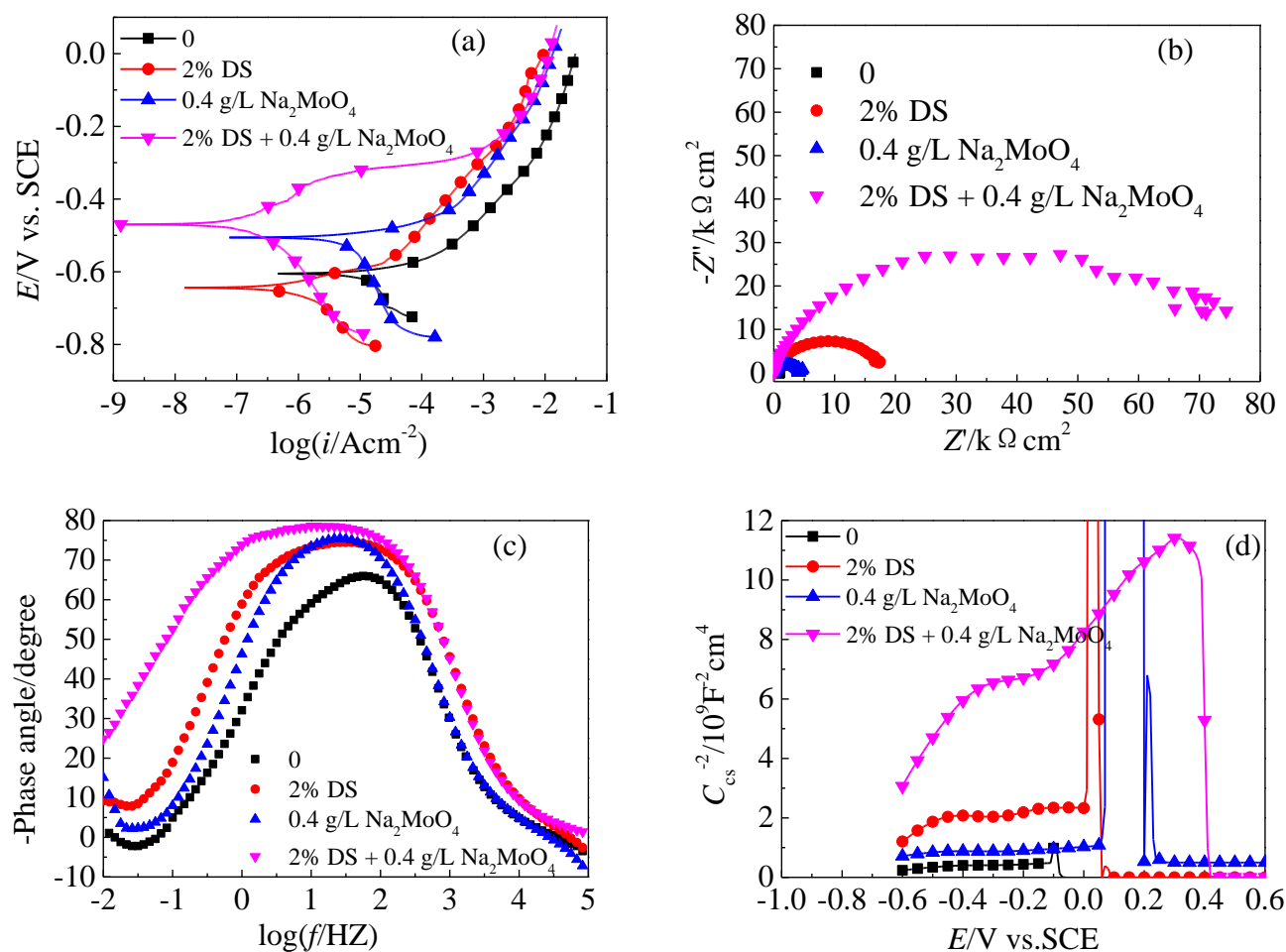


Figure 7. Effect of composite inhibitor of DS and molybdate on the polarization curves (a), Nyquist diagrams (b), Bode diagrams (c) and Mott-Schottky curves (d) for HRBF500 in SCP solutions containing 3.5% NaCl

Where $P_{e,DS}$ is the corrosion protection efficiency of 2% DS, of which is 96.3% (Table 1). $P_{e,the}$, $P_{e,Mo}$ and $P_{e,com}$ have been explained in the preceding paragraph. Thus, the $P_{e,the}$ value is 98.8%, less than the actual protection efficiency, 99.3%, of the composite inhibitor for HRBF500. It can be

concluded that a synergistic corrosion inhibition effect of the composite inhibitor, DS and molybdate, has been exerted.

As shown in Fig. 7 (b), the electrochemical impedance values of the HRBF500 samples increase in the following order: without inhibitor < with 0.4 g/L sodium molybdate < with 2% DS < with the composite inhibitor. Further, the impedance value for the composite inhibitor is far larger than the sum of that for the single molybdate plus DS, again confirming the synergistic effect of the composite inhibitor with respect to corrosion inhibition.

As shown in Fig. 7 (c), the peak of the negative phase angle for the composite inhibitor is obviously larger than those for the two single inhibitors, and the frequency range corresponding to the peak is also significantly broadened and shifted to the low frequency end. It indicates that the corrosion products on the surface of HRBF500 are more compact and thicker when the composite inhibitor was used.

As shown in Fig. 7 (d), the slope of the Mott-Schottky curve for the composite inhibitor is negative and contains two straight lines, similar to those obtained for the single DS. The corrosion products also have shallow and deep donor concentrations, i.e. N_{D1} and N_{D2} . Moreover, the discontinuous change on the Mott-Schottky curve, i.e., the depletion of donor concentrations, occurs when the electrode potential was up to 0.4 V, much higher than those for other curves. It can be concluded that the composite inhibitor promotes the transfer of Fe^{2+} to Fe^{3+} in the inner layer of the corrosion product membrane on the HRBF500 surface, significantly enhancing the corrosion resistance of HRBF500. This can be attributed to the presence of molybdate which is a strong oxidation inhibitor [45]. Based on the Mott-Schottky theory, the N_{D1} and N_{D2} values for the corrosion products formed in the presence of molybdate alone are $10.2 \times 10^{19} \text{ cm}^3$ and $19.3 \times 10^{19} \text{ cm}^3$, respectively. And those in the presence of the composite inhibitor are $0.829 \times 10^{19} \text{ cm}^3$ and $1.06 \times 10^{19} \text{ cm}^3$, far less than those for either DS or molybdate on their own.

The above results indicate that the anodic and cathodic corrosion of HRBF500 reinforcement in SCP solutions containing 3.5% NaCl can be significantly inhibited by the use of the composite inhibitor, 2% DS and 0.4 g/L sodium molybdate. The corrosion products are more compact and thicker and contain a higher content of Fe^{3+} . A synergistic effect on the corrosion inhibition is exerted by the composite inhibitor. The inhibition mechanism of the composite inhibitor will be explored in future studies.

4. CONCLUSIONS

The cathodic corrosion process of HRBF500 reinforcement in SCP solutions containing 3.5% NaCl can be obviously inhibited by DS inhibitor. With an increase in DS content from 0% to 2.0%, the corrosion current density decreases from $12.3 \mu\text{A} \cdot \text{cm}^{-2}$ to $0.45 \mu\text{A} \cdot \text{cm}^{-2}$ and the electrochemical impedance and the corrosion protection efficiency are greatly enhanced. The corrosion products are of the *n*-type semiconductor category and with a decrease in donor concentration. The corrosion of HRBF500 reinforcement is markedly reduced in the presence of DS. Nevertheless, the corrosion still exists.

In SCP solutions with 3.5% NaCl, the corrosion resistance of HPB300 reinforcement is superior to that of HRBF500. In the presence of 2% DS, the anodic polarization curve for HPB300 has a passivation zone and the impedance value is much greater than that for HRBF500. The corrosion inhibition efficiency of DS for HPB300 is better than that for HRBF500.

With respect to the corrosion inhibition effect of the composite corrosion inhibitor, DS and molybdate, on HRBF500, the electrochemical performance indexes are significantly enhanced relative to those used the single inhibitor. Moreover, the surface corrosion products are more compact and thicker, providing a better corrosion protection. The synergistic effect on the corrosion resistance of the composite inhibitor, DS and molybdate, was clearly demonstrated.

Great differences have been noted in the corrosion behavior of HRBF500 and HPB300 reinforcements in chloride-contaminated SCP solutions irrespective of whether the solutions contained corrosion inhibitors. Therefore, on the occasion of the extensive application of HRBF500 reinforcement and to ensure the durability and safety of the reinforced concrete structures, systematic investigations should be undertaken on the corrosion properties of HRBF500 reinforcement.

ACKNOWLEDGEMENTS

This work was financially supported by the National Nature Science Foundation of China (Nos. 51408517 and 51578255) and the Nature Science Foundation of Fujian Province (No. 2017J01489).

References

1. S. M. Haleem, E. E. Aal, S. Wanees and A. Diab, *Corros. Sci.*, 52 (2010) 3875.
2. J.O. Rivera-Corral, G. Fajardo, G. Arliguie, R. Orozco-Cruz and P. Valdez, *Constr. Build. Mater.*, 147 (2017) 815.
3. S. Abd El Wanees, A. Bahgat Radwan, M.A. Alsharif and S.M. Abd El Haleem, *Mater. Chem. Phy.*, 190 (2017) 79.
4. Y. S. Wang, Y. Zuo, X. H. Zhao and S. S. Zha, *Appl. Surf. Sci.*, 379 (2016) 98.
5. L. Abosrra, A. F. Ashour and M. Youseffi, *Constr. Build. Mater.*, 25 (2011) 3915.
6. T. U. Mohammed, N. Otsuki and M. Hisada, *J. Mater. Civil Eng.*, 13 (2001) 194.
7. T. U. Mohammed, N. Otsuki and M. Hisada, *Cement Concrete Res.*, 31(2001) 829.
8. M. P. Papadopoulos, C. A. Apostolopoulos and N. D. Alexopoulos, *Mater. Design*, 28 (2007) 2318.
9. J. H. Jiang, Y. S. Yuan, F. M. Li, B. Wang and Y. S. Ji, *J. Build. Mater.*, 12 (2009) 523.
10. O. Geng, Y. S. Yuan, F. M. Li, Q. Wu and J. D. Zhang, *J. China Min. Techno.*, 35 (2006) 488.
11. G. Li, X. M. Dalang and Y. S. Yuan, *J. China Min. Techno.*, 38 (2009) 149.
12. J. J. Shi, W. Sun and G. Q. Geng, *Acta Metall. Sin.*, 47 (2011) 449.
13. J. J. Shi, W. Sun, G. Q. Geng and P. Jiang, *J. Univ. Sci. Technol. B.*, 33 (2011) 1471.
14. B. L. Lin and Y. Y. Xu, *J. Zhenzhou Univ. Light Ind. (Natural Sci.)*, 25 (2010) 45.
15. B. L. Lin and Y. Y. Xu, *Int. J. Electrochem. Sci.*, 11 (2016) 3824.
16. B. L. Lin, C. N. Liu, Z. Luo, J. D. Li, S. Wang and Y. Y. Xu, *Int. J. Electrochem. Sci.*, 12 (2017) 2070
17. B. L. Lin and Y. Y. Xu, *J. Build. Mater.*, 19 (2016) 1082.
18. L. Yohai, W. Schreiner, M. Vázquez and M. B. Valcarce, *Electrochim. Acta*, 202 (2016) 231.
19. H. Nahali, L. Dhouibi and H. Idrissi, *Constr. Build. Mater.*, 50 (2014) 87.
20. R. J. Yang, Y. Guo, F. M. Tang, X. P. Wang, R. G. Du and C. J. Lin, *Acta Phys.-Chim. Sin.*, 28 (2012) 1923.
21. H. T. Zhai, *The preparation and application study of the environment-protecting inhibitor in the*

- inhibition of the metal*, Hefei Univ. Technol., 2008, Hefei, China.
22. M.M. Mennucci, E.P. Banczek, P.R.P. Rodrigues and I. Costa, *Cement Concrete Comp.*, 31 (2009) 418.
 23. F. L. Fei, J. Hu, J. X. Wei, Q. J. Yu and Z. S. Chen, *Constr. Build. Mater.*, 70 (2014) 43.
 24. S. B. Jiang, L. H. Jiang, Z. Y. Wang, M. Jin, S. Y. Bai, S. Q. Song and X. C. Yan, *Constr. Build. Mater.*, 150 (2017) 238.
 25. N. Gartner, T. Kosec and A. Legat, *Mater. Chem. Phys.*, 184 (2016) 31.
 26. H. Nahali, H. Ben Mansour, L. Dhouibi and H. Idrissi, *Constr. Build. Mater.*, 141 (2017) 589.
 27. K. Ma, Y. Z. Zhao, Y. H. Liu, X. Li and L. Mei, *Specialty Petrochemicals*, 32 (2015) 47.
 28. I. N. D. S. Corrêa, S. S. P. D. Silva, D. S. D. Queiroz, D. O. Rosas and M. A. P. Langone, *J. Mol. Catal. B-Enzym.*, 2016.
 29. Y. Xu, E. Z. Hu, K. H. Hu, Y. F. Xu and X. G. Hu, *Tribol. Int.*, 92 (2015) 172.
 30. Y. F. Chen, W. Wang and J. X. Yang, *J. Univ. Sci. Technol. B.*, 12 (2007) 21.
 31. W. Wang, *Development and mechanism research of steel bar rust inhibitor*, Northeast DianLi University, 2007, Changchun, China.
 32. Y. Guo, *Study on the depassivation of reinforcing steel and the inhibition effects of several inhibitors*, Xiamen University, 2013, Xiamen, China.
 33. R. G. Du, Y. Du, J. Zhang, X. P. Wang and C. J. Lin, *A composite corrosion inhibitor for reinforcing steel without nitrite*, 2012, CN102617062A, China.
 34. X. H. Li, S. D. Deng and H. Fu, *Corros. Sci.*, 53 (2011) 2748.
 35. X. Zhou, H. Y. Yang and F. H. Wang, *Corros. Sci., Protect. Technol.*, 22 (2010) 343.
 36. Y. Zhou, Y. Zuo and B. Lin, *Mater. Chem. Phys.*, 192 (2017) 86.
 37. T.J. Mesquita, E. Chauveau, M. Mantel, N. Kinsman, V. Roche and R.P. Nogueira, *Chem. Phys.*, 132 (2012) 967.
 38. M. A. G. Tommaselli, N.A. Mariano and S.E. Kuri, *Constr. Build. Mater.*, 23 (2009) 328.
 39. Y. Zhou and Y. Zuo, *Appl. Surf. Sci.*, 353 (2015) 924.
 40. C. N. Cao, *Principles of electrochemistry of corrosion*, Chemical Industry Press, 2008, Beijing, China.
 41. C. N. Cao and J. Q. Zhang, *Introduction of electrochemical impedance spectroscopy*, Science Press, 2004, Beijing, China.
 42. D.V. Ribeiro and J.C.C. Abrantes, *Constr. Build. Mater.*, 111 (2016) 98.
 43. A.V. Benedeti, P.T.A. Sumodjo, K. Nobe, P.L. Cabot and W.G. Proud, *Electrochem. Acta*, 40 (1995) 2657.
 44. N. Tang, W. J. V. Ooij and G. Górecki, *Prog. Org. Coat.*, 30 (1997) 255.
 45. Z. Brytan, J. Niagaj, Ł. Reiman, *Appl. Surf. Sci.*, 388 (2016) 160.
 46. D.V. Ribeiro and J.C.C. Abrantes, *Constr. Build. Mater.*, 111 (2016) 98.
 47. J. M. Yao, *College Physics*, Beijing Institute of Technology Press, 2008, Beijing, China.
 48. Q. Wu, W. Chen, R. G. Du, L. Sun and C. J. Lin, *J. Funct. Mater.*, 39 (2008) 764.
 49. J. Luo, Y. Wang, J. B. Jiang, Q. D. Zhong, Z. Y. Zhu and L. Zhang, *Acta Chim. Sin.*, 70 (2012) 1213.
 50. X. G. Chen, Y. Yang, Z. G. Lin, W. Chu, Y. X. Shi and B. M. Wei, *Appl. Surf. Sci.*, 103 (1996) 189.
 51. J. S. Kim, E. A. Cho and H. S. Kwon, *Corros. Sci.*, 43 (2001) 1403.
 52. W. Chen, R. G. Du, R. G. Hu, H. Y. Shi, Y. F. Zhu and C. J. Lin, *Acta Metall. Sin.*, 47 (2011) 735.
 53. T. Suzuki, H. Nishihara and K. Aramaki, *Corros. Sci.*, 38 (1996) 1223.